Cell Biochem Biophys (2017) 75:369–385
DOI 10.1007/s12013-017-0792-7

ORIGINAL PAPER

High Cholesterol/Low Cholesterol: Effects in Biological Membranes: A Review

Witold K. Subczynski[1] · **Marta Pasenkiewicz-Gierula**[2] · **Justyna Widomska**[3] · **Laxman Mainali**[1] · **Marija Raguz**[1,4]

Received: 20 January 2017 / Accepted: 27 March 2017 / Published online: 17 April 2017

Abstract Lipid composition determines membrane properties, and cholesterol plays a major role in this determination as it regulates membrane fluidity and permeability, as well as induces the formation of coexisting phases and domains in the membrane. Biological membranes display a very diverse lipid composition, the lateral organization of which plays a crucial role in regulating a variety of membrane functions. We hypothesize that, during biological evolution, membranes with a particular cholesterol content were selected to perform certain functions in the cells of eukaryotic organisms. In this review, we discuss the major membrane properties induced by cholesterol, and their relationship to certain membrane functions.

Keyword EPR · Oximetry · Lipid spin label · Membrane domains · Cholesterol

✉ Witold K. Subczynski
subczyn@mcw.edu

[1] Department of Biophysics, Medical College of Wisconsin, Milwaukee, WI, USA

[2] Department of Computational Biophysics and Bioinformatics, Jagiellonian University, Krakow, Poland

[3] Department of Biophysics, Medical University of Lublin, Lublin, Poland

[4] Department of Medical Physics and Biophysics, University of Split, Split, Croatia

Introduction

The most fundamental function of biological membranes is to enclose the cell and cellular organelles. That way, the plasma membrane maintains the essential differences between the cytosol and the extracellular environment, and the other intracellular membranes maintain the characteristic differences between the contents of each organelle and the cytosol. Membranes also provide the environment in which integral membrane proteins are located, specifically oriented, and specifically assembled. The strict separation of environments by biological membranes is largely due to the hydrophobicity of their interior. However, biological membranes enable communication and transport between the interior and exterior of the cell or the organelle. Water-soluble components such as ions and sugars can cross membranes by channels and transporters [1–3]. Nonelectrolytes can directly permeate the lipid bilayer membrane portion by passive diffusion [4]. Specific assemblies of membrane proteins allow membranes to perform the most complex functions such as signal transduction [5–7] and energy transformation [8]. Nevertheless, the lipid-bilayer portion of the biological membrane determines bulk membrane properties (including diffusion barriers [9, 10]) and can affect the functioning of membrane proteins [11–14].

In this review, we assert that the diversity in the lipid composition determines the membrane properties that allow the membranes to perform certain cellular functions. Cholesterol (Chol) plays a major role in this determination. Thus, we will concentrate mainly on the role of Chol in modifying the main properties of the lipid bilayer of biological membranes such as fluidity, permeability, and hydrophobicity (dielectric properties), and also on its role in the formation of separated phases and domains in the bilayer. The major hypothesis, which we will support thorough this review, states that during

biological evolution, membranes with a particular Chol content were selected to perform certain functions in the cells of eukaryotic organisms. Parallel with membrane evolution, the structure of the Chol molecule evolved over a very long time to obtain the ability to optimize certain physical properties of cell membranes with regard to biological functions [15, 16]. In effect, the Chol structure is optimal for its interactions with other lipid species [17, 18]. Like other membrane lipids, Chol is amphiphilic; however, its structure—a rigid fragment that has a smooth side and a rough side, and a short hydrocarbon chain—differs significantly from that of other lipid species of eukaryotic cell membranes.

The long-standing opinion is that the Chol content in the eukaryotic cell membranes increases along the secretory pathway, being very low in the endoplasmic reticulum, higher in the Golgi apparatus, and highest in the plasma membrane [19, 20]. Indeed, this is confirmed when the Chol contents in these biological membranes are compared. The first group comprises the endoplasmic reticulum, Golgi apparatus, and mitochondria membranes, all of which have a *low Chol content*, with a Chol-to-phospholipid (PL) molar ratio between 0 and 0.1 (<10 mol% Chol). Data for these membranes are scattered, but they indicate that, for the endoplasmic reticulum and Golgi apparatus, the Chol/PL molar ratios are as low as 0.06 and 0.1, respectively [21] (see, however, ref. [20] for Chol content in Golgi apparatus). The second group comprises biological membranes with a *normal Chol content* (this is our terminology), which are typical plasma membranes with a Chol/PL molar ratio between 0.1 and 0.5 (from 10 to 30 mol% Chol) [22]. Even though most of the cellular plasma membranes show such Chol content, the content in certain cells is significantly higher. The third group, which comprises membranes with a *high Chol content*, includes the plasma membrane of red blood cells and the myelin membranes of Schwann cells isolating nerve axons; the Chol/PL molar ratio in these membranes is close to 1 (~ 50 mol% Chol) [23, 24]. At a Chol/PL molar ratio of 1, Chol saturates the PL bilayer [25]. In membranes with a greater Chol content, Chol starts to form immiscible pure Chol domains, called Chol bilayer domains (CBDs), within the PL bilayer saturated with Chol [26]. We refer to membranes in which CBDs are present as having *very high Chol content*. This fourth group comprises fiber cell plasma membranes of the eye lens, especially those of human eyes, for which the Chol/PL molar ratio is greater than 1 (>50 mol% Chol) [27–29]. When the Chol content exceeds the Chol solubility threshold (CST), usually at a Chol/PL molar ratio of 2 (66 mol% Chol), Chol crystals are formed, presumably outside the lipid bilayer [25, 30]. This situation can be observed in the clear human eye lenses of old individuals as well as in the membranes of atherosclerotic arteries [30–32]. We call this situation *Chol content beyond the CST*.

PLs are the most basic molecular components of a biological membrane. They form the lipid bilayer in which integral membrane proteins are immersed. At physiological temperatures, all membrane components undergo thermal diffusion. If the membrane were to follow the fluid-mosaic model [33], the diffusional motion would be laterally unrestricted, and all membrane components would be uniformly mixed; in effect, the membrane would constitute a homogeneous and featureless bilayer structure. But the membrane is not such [34], which strongly suggests that the fluid-mosaic model is not entirely correct, even though it can describe some membrane functions [35–37]. In the membrane, lipid-lipid, lipid-protein, and protein-protein interactions lead to the formation of domains that play an essential role in the functioning of biological membranes. The relationship between the different types of domains and membrane functions is one of the key issues of membrane biology today.

As previously mentioned, Chol plays a key role in the lateral organization of the lipid bilayer and the determination of basic membrane properties. The Chol molecule contains three well-distinguished regions: a small polar hydroxyl group, a rigid plate-like steroid ring, and a flexible isooctyl chain. Chol intercalates into the membrane with a polar hydroxyl group positioned between the PL polar headgroups, and its rigid, plate-like ring structure reaches the depth of the C9–C10 carbon atoms of the PL acyl chains. The Chol isooctyl chain, the cross section of which is much smaller than that of the rigid ring, is located in the membrane center. Chol affects membrane properties differently at different depths [38–40].

In this review, the effect of Chol on the PL bilayer is illustrated with bilayers made of dimyristoylphosphatidylcholine (DMPC) and Chol. We will also demonstrate that the electron paramagnetic resonance (EPR) spin-labeling approaches can provide unique information about the lateral organization of the lipid bilayer membranes, allowing discrimination of membrane phases and domains in situ, without their physical separation. EPR spin-labeling methods also provide a number of unique approaches for determining several important membrane properties as a function of the bilayer depth. Because this issue of *Cell Biochemistry and Biophysics* is dedicated to the applications of EPR in biomedical research, we will also provide a short explanation of how this type of information about membrane properties and organization can be obtained from EPR signals.

Phases and Domains

The phase diagram for the DMPC/Chol mixture together with the schematic drawings shown in Figure 1 are used to

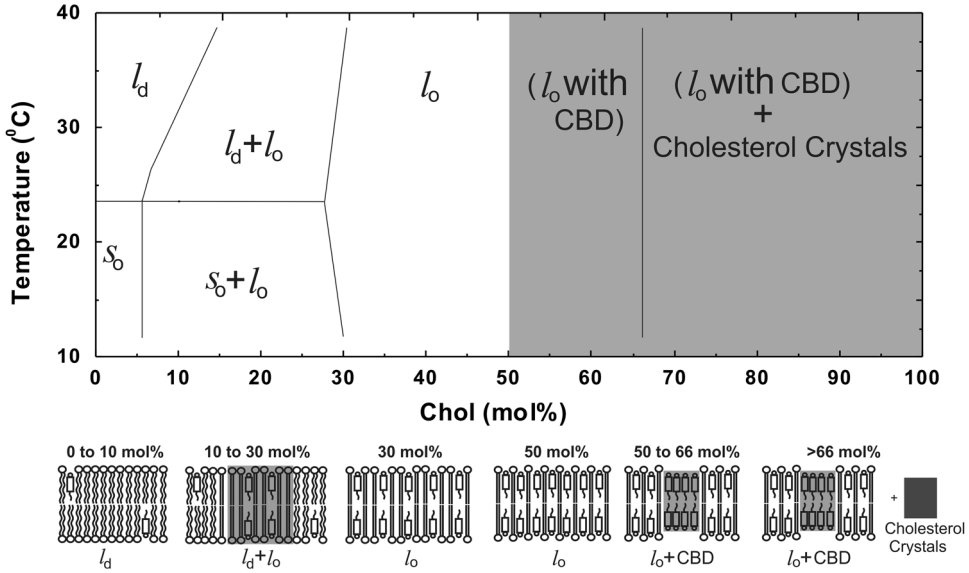

Fig. 1 Phase diagram for DMPC/Chol mixtures is reproduced from ref. [25], Copyright 2013, with permission from American Chemical Society. The *shaded area* indicates the region where CBDs are detected, forming the structured l_o phase of DMPC membranes. Between 50 and 66 mol% Chol is a structured, one-phase region (dispersed phase region) where CBDs are supported by the DMPC bilayer saturated with Chol. The phase boundary at 66 mol% Chol separates the structured, one-phase region from the two-phase region (structured l_o phase of DMPC and Chol crystals). It should be noted that the phase rule has to be obeyed for all regions and phase boundaries: $f = c - p + 1$ (f, degree of freedom; c, number of components; p, number of phases, assuming that the pressure is constant for membranes). Schematic drawings of membrane structures (including phases, domains, and crystals) formed at a different Chol content in the DMPC/Chol mixture. l_d, liquid-disordered phase; l_o, liquid-ordered phase; s_o, solid-ordered phase; CBD, Chol bilayer domain; Chol crystals, monohydrated Chol crystals

illustrate how membrane organization changes with Chol content, in order to help guide readers through this review. The DMPC/Chol bilayer forms one of the simplest paradigms for the study of formation, coexistence, and separation of phases and domains (see [41] for an extended terminological discussion regarding "phases" and "domains"). The phase diagram in Fig. 1 indicates single-phase regions of liquid-disordered (l_d) and solid-ordered (s_o) phases (separated by the main phase transition at 23.6 °C) between 0 and ~ 10 mol% Chol and that of the liquid-ordered (l_o) phase between ~ 30 and 50 mol% Chol. In the region of Chol content between ~ 10 and ~ 30 mol%, two phases coexist, l_d and l_o (above the phase transition temperature) and s_o and l_o (below the phase transition temperature). At a Chol content above 50 mol%, the l_o phase becomes a structured l_o phase (see [42] for terminology) because the excess Chol forms CBDs within the l_o phase [25]. In the terminology of Simons and Vaz [43], such a region can be called a dispersed phase. Chol crystals do form at 66 mol% Chol (CST for DMPC [44]) and, even if the Chol exchange between the crystal and the bilayer pool is too slow to be observed, Chol crystals represent an equilibrium state of Chol [41]. The two-phase region above the 66 mol% Chol contains both Chol crystals and a structured l_o phase.

The phase diagrams per se do not tell us much about the structure and properties of the single or coexisting phases. However, we can get significant information about Chol distribution between these phases at the particular Chol mixing ratio at which membranes were prepared (at a certain Chol content). In any phase, the Chol concentration has an upper limit that can be accommodated within the phase. For a DMPC/Chol mixture at 27 °C, the limit for the l_d phase is 6 mol% Chol, above which the excess Chol forms an l_o phase (with a Chol concentration of 27 mol%). The upper limit of the Chol concentration in the l_o phase of the DMPC membrane is 50 mol%, above which the excess Chol forms CBDs. The next limit is defined by the CST; above this limit, Chol crystals are formed. The phase diagrams also do not indicate if each of the two coexisting phases is dispersed into one larger domain or into a number of smaller domains.

EPR Approach

In EPR studies of lipid bilayers, both PL-analog (1-Palmitoyl-2-(n-doxylstearoyl) phosphatidylcholine (n-PC) and n-doxylstearic acid spin labels (n-SASL)) and Chol-analog (androstane spin label (ASL) and cholestane spin label (CSL)) spin labels were used. The structures of the most commonly used spin labels are presented in Fig. 2. These spin labels, when introduced to the investigated membranes, give rise to the EPR signal at specific membrane depths and

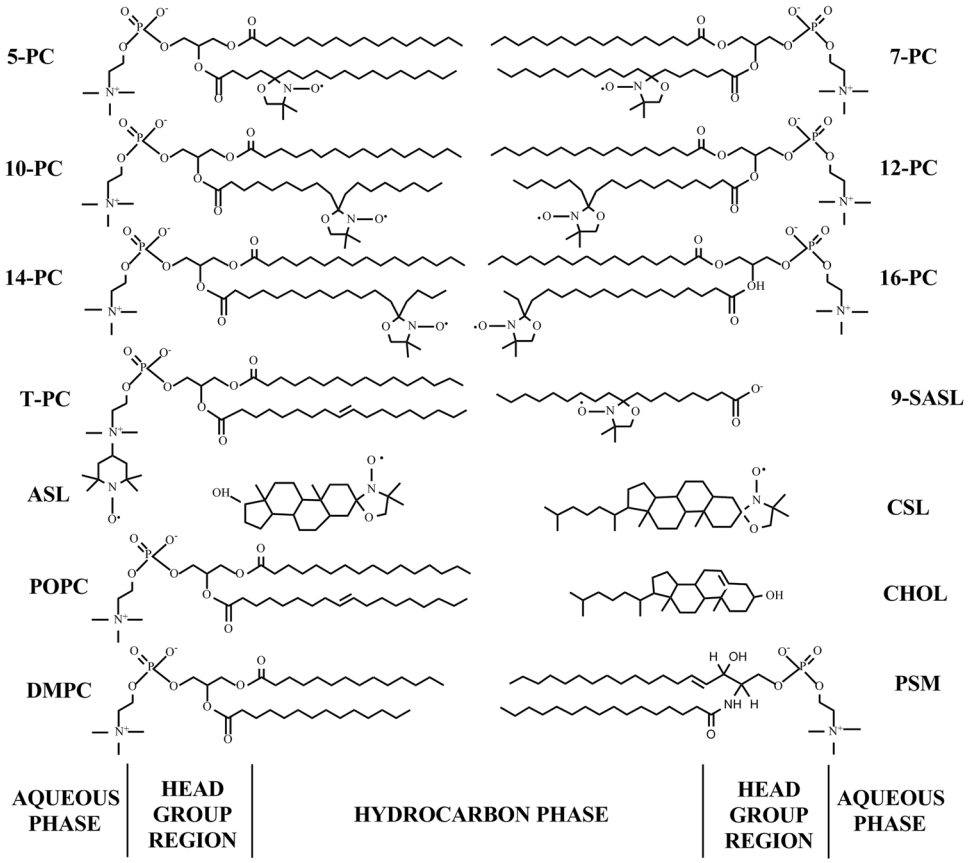

Fig. 2 Chemical structures of PL-(n-PC and tempocholine-1-palmitoyl-2-oleoylphosphatidic acid ester (T-PC)), stearic acid-(n-SASL), and Chol-analog spin labels (ASL and CSL) together with the structure of Chol (CHOL), DMPC, 1-palmitoyl-2-oleoylphosphatidylcholine (POPC), and palmitoyl sphingomyelin (PSM). POPC is a major PL of bioloical membranes and PSM is a major PL of the fiber cell plasma membranes in human eye lenses. Approximate locations of these molecules across the lipid bilayer are illustrated

in specific membrane domains. Applying both conventional and time-domain techniques, the dynamic state of the lipid molecules as well as the physicochemical properties of the microenvironment in the immediate vicinity of the nitroxide can be characterized. The spin labels, due to their respective overall similarity to PLs and Chol, are believed to be distributed between different membrane phases and domains, similar to PLs and Chol (see Fig. 1 for membrane domains and phases). The locations of spin labels in phases and domains consisting of molecules of corresponding structures allow the phases and domains to be discriminated and, in some cases, certain transmembrane profiles for coexisting membrane domains or coexisting membrane phases to be obtained without the need for their physical separation.

Below, we provide a detailed description of how the transmembrane profiles of some EPR spectral parameters describing certain membrane properties, such as acyl chain order, fluidity, hydrophobicity, and oxygen diffusion-concentration product (oxygen transport parameter [OTP]), can be obtained. Conventional EPR spectroscopy provides the order parameter and hydrophobicity profiles, whereas the time-domain saturation-recovery (SR) EPR method, which is highly sensitive to the rotational motion of the nitroxide moiety and to collisions between nitroxide and molecular oxygen, provides profiles of the membrane fluidity and OTP. Below, the profiles are grouped into those illustrating the order and the rotational motion of the PL acyl chains and those illustrating hydrophobicity and the diffusion-concentration products of oxygen. We will show how these profiles change as a function of the Chol content in the membrane.

Order of PL Acyl Chains

In lipid bilayers, an acyl chain of a PL-analog spin label (n-PC or n-SASL, Fig. 2) undergoes rapid anisotropic rotational motion due to its elongated shape and the axial symmetry of the lipid bilayer. It rotates about its long axis, and its long axis wobbles within the confines of a cone imposed by the membrane environment. However, because the acyl chain is flexible, each of its segments has its own rotational freedom, which gives rise to the unique features of the EPR spectrum [45]. From this spectrum, the order parameter for the spin labeled acyl chain segment can be calculated (Fig. 3a).

The order parameter is a measure of the amplitude of the wobbling motion of the given chain segment averaged over time and ensemble; thus, it can be considered a nondynamic parameter. However, profiles of the order parameter (Fig. 3b) have been routinely used as a measure of the

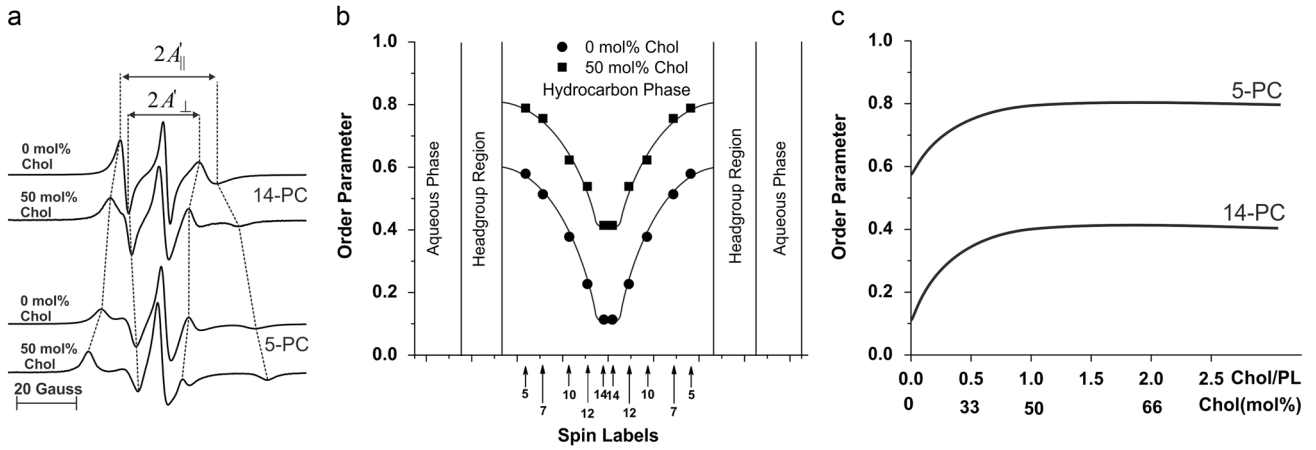

Fig. 3 Order parameter (amplitude of the wobbling of the acyl chain segment). **a** Representative EPR spectra from 5- and 14-PC in DMPC membranes in the absence and presence of 50 mol% Chol recorded at 27 °C. Measured values for evaluating order parameters are indicated. The order parameter S was calculated according to Marsh [45] using the equation $S = 0.5407\left(A'_{\parallel} - A'_{\perp}\right)/a_0$, where $a_0 = \left(A'_{\parallel} + A'_{\perp}\right)/3$. **b** Profiles of the order parameter obtained with n-PCs at 27 °C for DMPC membranes in the absence and presence of 50 mol% Chol. Approximate localizations of the nitroxide moieties of spin labels are indicated by *arrows*. **c** Order parameter of 5-PC and 14-PC in DMPC membranes plotted as a function of the mole fraction of Chol for measurements made at 27 °C. *Curves* represent averages of the values obtained from various experiments and show qualitative dependence of the indicated parameter on the Chol bilayer content

membrane fluidity [46, 47]. As shown in Fig. 3b, when the spin label moiety is moved down along the acyl chain, the effect of the wobbling (a decrease of the chain order parameter) accumulates. The effect of accumulation is clearly demonstrated by the shape of the order parameter profiles for bilayers containing Chol (Fig. 3b). The Chol ring induces ordering not only of the acyl chain segments in direct contact with the ring (close to the membrane surface) but also of the distal segments (close to the membrane center). Thus, as shown in Fig. 3b, the ordering of acyl chains by Chol proceeds from the membrane surface to the membrane center. This effect has also been observed in computer simulation studies of the DMPC/Chol bilayers, e.g., ref. [48].

As indicated by the phase diagram and schematic drawings presented in Fig. 1, at increased Chol content, the coexisting phases and domains are present in the DMPC bilayer. However, using the conventional EPR spectra of spin labels, one cannot discriminate these phases and domains. Order parameters derived from these spectra are averaged over spin labels located in the coexisting phases and domains. However, as PL-analog spin labels are located only in PL/Chol phases, the profiles obtained with these spin labels are not contaminated by the CBD. As follows from the phase diagram in Fig. 1, this is true for Chol content in the DMPC bilayer greater than 50 mol%.

The values of the order parameter of acyl chains close to the membrane surface (C5 position, data obtained with 5-PC) and in the membrane center (C14 position, data obtained with 14-PC) are presented in Fig. 3c as a function of Chol content in the DMPC bilayer. As shown in Fig. 3c, at both locations, the order parameter continuously increases with Chol content, up to the Chol/DMPC molar ratio of 1, and then becomes constant upon further increases in Chol. This makes sense because, above the Chol/DMPC molar ratio of 1 (50 mol% Chol), CBDs start to form within the DMPC/Chol bilayer, which remains saturated with Chol even though Chol content increases above 50 mol%. This agrees with the phase diagram presented in Fig. 1. Further increases in Chol beyond the CST (66 mol% Chol) cause formation of Chol crystals. Their formation does not affect the values of the order parameter for the same reasons as discussed with regard to CBD formation. These results may lead to the conclusions that (1) CBDs can be supported by the surrounding DMPC bilayer saturated with Chol when Chol content is between 50 and 66 mol% (Chol/PC molar ratio between 1 and 2), and (2) as shown in ref. [25], formation of CBDs precedes formation of Chol crystals.

Fluidity of The Bilayer

In our previous papers, we proposed use of the spin-lattice relaxation rate (T_1^{-1}, the inverse of the spin-lattice relaxation time T_1) as a convenient quantitative measure of local membrane dynamics commonly termed fluidity [49, 50]. In a deoxygenated spin labeled lipid bilayer, T_1^{-1} depends primarily on the rate of rotational motion of the nitroxide moiety [51, 52] and thus describes the dynamics of the acyl chain fragment to which the nitroxide moiety is rigidly attached. As shown in Fig. 4a, T_1 can be obtained from SR EPR measurements, allowing studies of the effects of membrane modifiers, like Chol, on membrane fluidity. T_1^{-1} measured for n-SASL or n-PC spin labels provides a fluidity profile across the lipid bilayer. The profiles across DMPC

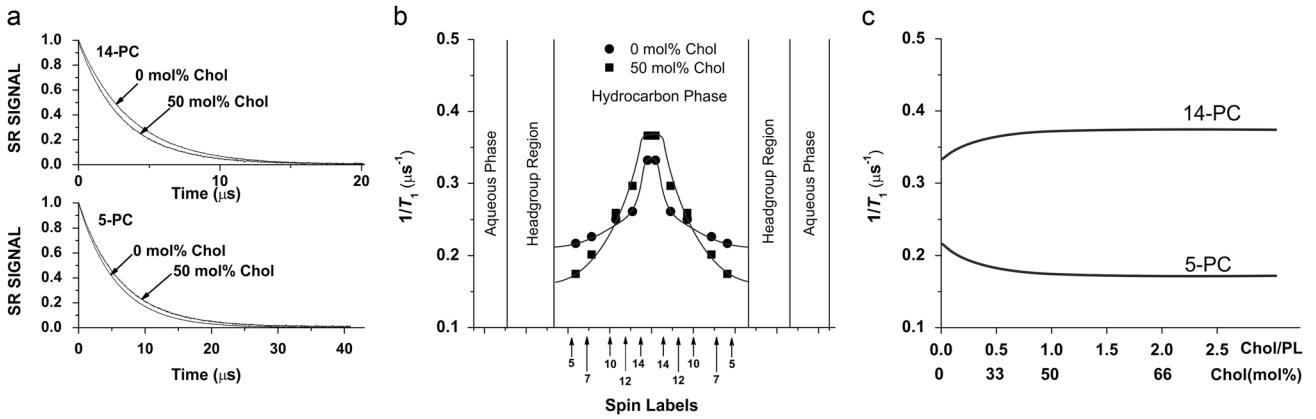

Fig. 4 Membrane fluidity (spin-lattice relaxation rate T_1^{-1}). **a** Representative SR signals with fitted curves from 5- and 14-PC in DMPC membranes in the absence and presence of 50 mol% Chol recorded at 27 °C. Signals were recorded for deoxygenated samples (equilibrated with 100% nitrogen). The SR signals can be satisfactorily fitted only with a single exponential function (see details in [49]): for 5-PC in the absence and presence of 50 mol% Chol, with time constants (T_1) of 4.61 ± 0.01 and 5.73 ± 0.01 μs, respectively, and for 14-PC in the absence and presence of 50 mol% Chol, with time constants of 3.01 ± 0.01 and 2.73 ± 0.01 μs, respectively. **b** Profiles of T_1^{-1} (the spin-lattice relaxation rate) obtained for n-PC spin labels at 27 °C for DMPC membranes in the absence and presence of 50 mol% Chol. Approximate localizations of the nitroxide moieties of spin labels are indicated by arrows. **c** T_1^{-1} of 5- and 14-PC in DMPC membranes plotted as a function of the mole fraction of Chol for measurements made at 27 °C. *Curves* represent averages of the values obtained from various experiments and show qualitative dependence of the indicated parameter on the Chol bilayer content

bilayers without and with 50 mol% Chol are shown in Fig. 4b. As expected, for both systems, moving the spin label position progressively deeper into the bilayer increases the value of T_1^{-1}, which corresponds to an increase in membrane fluidity (membrane dynamics). However, comparison of the profiles for DMPC and DMPC with 50 mol% Chol bilayers indicates that in the presence of Chol the membrane fluidity decreases close to the bilayer surface and increases near the bilayer center. The transition between the rigidifying and fluidizing effects of Chol lies approximately at the position of the C9 carbon atom, the depth to which the rigid Chol ring is immersed into the bilayer. These results are in accordance with atomistic computer simulation studies that show the exact positions of the Chol ring atoms and the effect of the Chol ring on packing of the atoms in the DMPC/Chol bilayer, refs [18, 53, 54]. Here, we would like to stress that profiles of the order parameter do not differentiate the effects of Chol at different depths (cf. Fig. 3b) as they show that the Chol ordering effect extends to all bilayer depths.

Effects of Chol on membrane fluidity close to the membrane surface (at the C5 position) and in the membrane center (at the C14 position) are summarized in Fig. 4c. Close to the surface, Chol decreases membrane fluidity up to the Chol/DMPC molar ratio of 1. Similarly, in the membrane center, Chol increases membrane fluidity up to the Chol/DMPC molar ratio of 1. A further increase in Chol content does not affect membrane fluidity at any bilayer depth. As indicated above, n-PC and n-SASL spin labels are located only in the DMPC/Chol bilayer phases and, thus, report only on their fluidity, which is not affected by the presence of CBDs or by Chol crystals, formed presumably outside the membrane. T_1s obtained from SR EPR signals of T-PC (Fig. 2) with the nitroxide moiety located in the bilayer polar headgroup region of the DMPC and DMPC with 50 mol% Chol bilayers indicate that Chol increases membrane fluidity in this region [49, 50]. Because the structure of the nitroxide moiety of T-PC is different from that of n-PC and n-SASL, we cannot include the data obtained with T-PC in Fig. 4; however, the effect of Chol on the fluidity of the bilayer headgroup region is unequivocal. Increased fluidity in the headgroup region of the DMPC/Chol bilayer relative to that of the DMPC bilayer can be explained by increased motional freedom of the DMPC phosphorylcholine group resulting from increased spacing among DMPC molecules induced by the presence of Chol molecules in the bilayer, as was shown in a computer simulation study [55].

Results obtained for the order parameters (Fig. 3b and c) and for the membrane fluidity, T_1^{-1}, (Fig. 4b and c) might at first seem at variance. However, as noted above, the rigid sterol ring of Chol extends only to a depth of approximately the position of the C9 carbon atom in the acyl chains. Below the sterol ring, the Chol isooctyl chain has a cross section much smaller than that of the sterol ring; in effect, the central region of the bilayer is less dense than in the bilayer without Chol. This smaller density in the center of the DMPC/Chol bilayer can be seen from mass density profiles across the DMPC and DMPC/Chol bilayers in ref. [18], as well as from the molecular order parameter profile in ref. [56]. The order parameter is a cumulative quantity, even though it is measured locally. In the DMPC bilayer, the

rigid ring of Chol acts as a "wall," confining the wobbling of the chain fragments within its vicinity [48]; however, the "wall effect" is felt by all fragments of the chains due to the cumulative nature of the order parameter. In contrast are T_1^{-1} reports on the local motional state of a chain fragment that is practically independent of the motional states of other fragments. In the vicinity of the steroid ring, the packing of DMPC chains is tighter [54], so both the rate and the amplitude of the wobbling is diminished. However, in the less-dense environment of the DMPC/Chol bilayer center, the terminal fragments of the DMPC acyl chains rotate faster because they have a greater motional freedom. Thus, the increased mobility induced by Chol in the membrane center, indicated by the dynamic parameters describing the rate of motion, is consistent with an increased order parameter, describing the amplitude of motion.

Hydrophobicity of The Membrane Interior

The hydrophobicity of the membrane interior is largely determined by the extent of water penetration into the membrane. The membrane environment becomes increasingly nonpolar proceeding from the membrane surface to the termini of the lipid acyl chains. The pioneering work of Griffith et al. [57, 58] demonstrated, using EPR spin-labeling approach, the existence of a hydrophobicity gradient across the membrane. Since then, this method has been used intensively to study the hydrophobicity of the membrane interior [59, 60]. The EPR spin-labeling method is based on the solvent-polarity dependence of the unpaired electron's spin density at the nitrogen atom. Polar solvents enhance the density, thereby increasing the hyperfine interaction between the unpaired electron spin and the nitrogen nuclear spin. With an increase in solvent polarity, the z component of the hyperfine interaction, A_Z, increases. In membranes, this parameter, measured as a maximum splitting ($2A_Z$), may also be influenced by spin-label motion that averages the anisotropy of the A and g tensors. Because of that, and to eliminate the motional contribution, the hydrophobicity measurements are typically performed on samples in the frozen state, using $2A_Z$ (Fig. 5a) as a convenient experimental observable.

The hydrophobicity profiles for the DMPC and DMPC with 50 mol% Chol bilayers are shown in Fig. 5b. In the absence of Chol, bilayer hydrophobicity gradually increases toward the bilayer center and has a typical bell-shaped profile. Chol has dramatic effects on the hydrophobicity profile as it induces a decrease in hydrophobicity in the region close to the membrane surface, and a significant increase in hydrophobicity in the central region of the bilayer [59]. The hydrophobicity sharply increases between the C9 and C10 carbon atoms and then becomes flat. This very sharp increase occurs within a narrow range of one carbon-carbon bond (i.e., 1.34–1.53 Å). At positions below (i.e., deeper than) the C10 atom, $2A_Z$ values are almost constant, indicating a region of homogeneously high hydrophobicity. These give the hydrophobicity profile an overall rectangular shape.

Effects of Chol on membrane hydrophobicity close to the membrane surface (at the C5 position) and in the membrane center (at the C14 position) are summarized in Fig. 5c. Close to the surface, Chol decreases membrane hydrophobicity up to the Chol/DMPC molar ratio of 1. However, in the membrane center, Chol increases membrane hydrophobicity up to the Chol/DMPC molar ratio of 0.5 (~ 30 mol%). The further increase of Chol content does not affect membrane hydrophobicity, or slightly (within the error of measurement) decreases it. Measured values, both close to the membrane surface and in the membrane center, stabilize at the Chol/DMPC molar ratio of 1.

To give a physical meaning to the hydrophobicity measured as $2A_Z$ and indicated in Fig. 5a, its values for selected depths in the membrane were related to the polarity (or dielectric constant, ε) of bulk organic solvents in which $2A_Z$ of the dissolved spin label were similar, as shown in Fig. 2 in ref. [59]. Thus, for the DMPC bilayer, the addition of 50 mol% Chol increased polarity (decreased hydrophobicity) near the membrane surface (at the C5 positions) from that of 2-propanol ($\varepsilon = 15$) to that of methanol ($\varepsilon = 50$); the latter is high but indicates that this region is still considerably less polar than the bulk aqueous phase ($\varepsilon = 80$). Conversely, incorporation of 50 mol% Chol into the DMPC bilayer decreases polarity (increases hydrophobicity) in the middle of the bilayer from that of 2-pentanol or 1-octanol ($\varepsilon =$ 10–20) to the level of hexane ($\varepsilon = 2$). Here, we would like to stress that, in the PL bilayer, the hydrophobicity of the membrane interior depends on PL species, especially on PL unsaturation [59]. Saturated bilayers do not form high hydrophobic barriers; the hydrophobicity in their center is close to that of 2-pentanol or 1-octanol ($\varepsilon = 10$–20) while that in the center of unsaturated bilayers is close to that of 1-decanol ($\varepsilon = 10$, 1-palmitoyl-2-oleoylphosphatidylcholine, POPC). All these differences are canceled at saturating Chol contents because, for all bilayers, the hydrophobicity in the bilayer center is close to that of hexane ($\varepsilon = 2$).

OTP (Discrimination of Membrane Phases and Domains)

Bimolecular collisions of a nitroxide moiety of the spin label with molecular oxygen induce spin exchange, enhancing spin-lattice relaxation of the nitroxide. This effect can be measured directly using SR EPR (Fig. 6a). An OTP was introduced as a convenient quantitative measure of the collision rate between the spin label and molecular oxygen by Kusumi et al. [61] and is determined

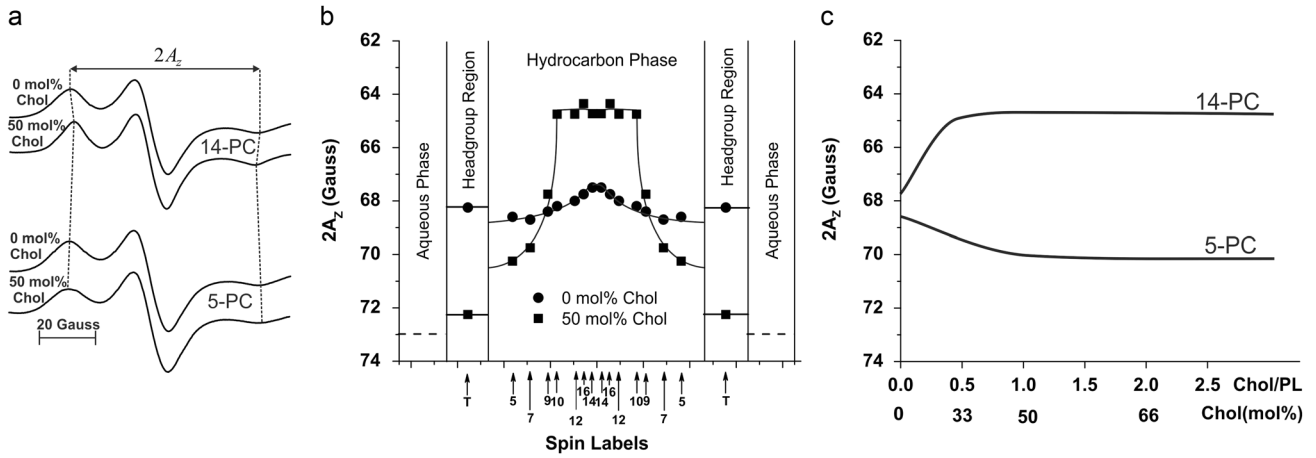

Fig. 5 Hydrophobicity (measured as the hyperfine interaction, $2A_Z$). **a** Representative EPR spectra of 5- and 14-PC from DMPC membranes in the absence and presence of 50 mol% Chol, recorded at −165 °C to cancel motional effects. The measured $2A_Z$ value is indicated. (For more details, see [59]). **b** Profiles of the hydrophobicity ($2A_Z$) obtained with n-PCs and 9-SASL for DMPC membranes in the absence and presence of 50 mol% Chol. Approximate localizations of the nitroxide moieties of spin labels are indicated by arrows. **c** $2A_Z$ of 5- and 14-PC in DMPC membranes plotted as a function of the mole fraction of Chol. *Curves* represent averages of the values obtained from various experiments and show qualitative dependence of the indicated parameter on the Chol bilayer content. Fig. 5b is reproduced from ref. [59], Copyright 1994, with permission from American Chemical Society

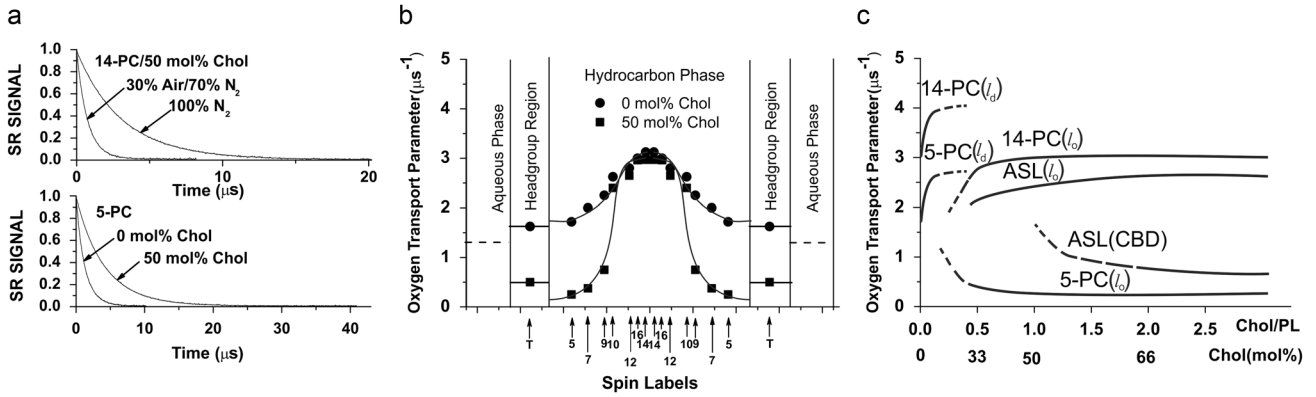

Fig. 6 Oxygen diffusion-concentration product (OTP). **a** Representative SR signals with fitted curves from 14-PC in DMPC membranes in the presence of 50 mol% Chol. Signals were recorded at 27 °C for samples equilibrated with 100% nitrogen and a gas mixture of 30% air/70% nitrogen. These SR signals can be satisfactorily fitted with a single exponential function: for 14-PC in pure DMPC, with time constants $T_1(N_2)$ of 3.01 ± 0.01 μs and T_1(30% air) 0.79 ± 0.01 μs. The OTP $W(x)$ was calculated according to Kusumi et al. [61] using the equation $W(x) = T_1^{-1}(\text{Air},x) - T_1^{-1}(N_2,x) \sim D(x)C(x)$. Here, x is the "depth" in the membrane. Note that the OTP is defined for samples equilibrated with air, so appropriate extrapolation should be done. Representative SR signals with fitted curves from 5-PC in DMPC membranes in the absence and presence of 50 mol% Chol. Signals were recorded at 27 °C for samples equilibrated with a 30% air/70% nitrogen gas mixture. SR signals can be satisfactorily fitted with a single exponential function: for 5-PC in pure DMPC, with a time constant T_1(30% air) of 1.36 ± 0.01 μs and for 5-PC in DMPC containing 50 mol% Chol, with a time constant T_1(30% air) of 4.01 ± 0.01 μs. Appropriate SR signals for 5-PC for deoxygenated samples are presented in Fig. 4a. **b** Profiles of the OTP obtained with n-PCs and 9-SASL for DMPC membranes in the absence and presence of 50 mol% Chol. Approximate localizations of the nitroxide moieties of spin labels are indicated by arrows. **c** OTP of 5- and 14-PC in DMPC membranes plotted as a function of the mole fraction of Chol for measurements made at 27 °C indicate the region (between ~10 and ~30 mol% Chol) where l_d and l_o phases coexist. Data obtained with ASL indicate the region (>50 mol% Chol) where the l_o phase contains CBDs. *Curves* represent averages of the values obtained from various experiments and show qualitative dependence of the indicated parameter on the Chol bilayer content. *Broken lines* indicate that the amount of the phase or the domain change from zero to the maximal value. Fig. 6b is reproduced from ref. [39], Copyright 2007, with permission from Elsevier

by calculating the difference between the spin-lattice relaxation rates of spin labels in samples equilibrated with air and nitrogen. The parameter is proportional to the product of the local translational diffusion coefficient and the local concentration of oxygen at the bilayer depth where the nitroxide moiety is located. By convention, the OTP is normalized to an oxygen concentration corresponding to the sample equilibrated with atmospheric air. To obtain the OTP, in principle, two SR measurements have to be performed: one for the sample equilibrated with

nitrogen and the other for the sample equilibrated with air (see Fig. 6a).

We will demonstrate the ability of this approach using OTP profiles obtained with PL-analog spin labels in the DMPC and DMPC with 50 mol% Chol bilayers as an example (Fig. 6b). The effect of Chol on the OTP is very different at different membrane depths (Fig. 6b). Chol changes the bell-shaped profile, observed for PL bilayers, to a rectangular-shaped profile. OTP abruptly increases between the positions of the C9 and C10 carbon atoms, that is, at the depth to which the rigid tetracyclic Chol structure is immersed. This abrupt increase is as large as ~threefold, and the overall change of the OTP across the DMPC/Chol bilayer becomes as large as ~fivefold. In the presence of Chol, the OTP in the region between the membrane surface and the position of the C9 carbon atom becomes as low as in the gel-phase PC bilayers; at locations deeper than the C9 carbon atom, it becomes as high as in the fluid-phase bilayers [40, 62]. The OTP profiles, similar to the hydrophobicity profiles, are significantly different for different PL membranes. However, saturation of PL membranes with Chol makes these profiles very similar in shape (rectangular) and values of the OTP.

The OTP makes it possible to discriminate different membrane domains because even small differences in the lipid packing of these domains can affect the partitioning and diffusion of molecular oxygen. Information about different packings of lipids is recorded in the SR signal. For membranes equilibrated with air and consisting of two lipid environments with different oxygen diffusion-concentration products, the SR signal is a simple double-exponential curve with two time constants. This is the basis of the SR EPR discrimination by oxygen transport (DOT) method [63, 64], which is used to detect and characterize coexisting phases and domains in the membrane [26, 39, 65–67]. Because membranes, and thus membrane domains, do not have uniform properties across themselves (and may be viewed as three-dimensional structures), knowledge of the molecular events in the depth dimension is important. The DOT method not only shows the lateral organization of lipid membranes or differentiate between membrane domains, but also provides information about molecular dynamics and structure in the third dimension, namely, in the direction perpendicular to the bilayer surface. We demonstrated that the DOT method, with the use of PL-analog spin labels, can distinguish and characterize l_o, l_d, and s_o phases in different regions of a phase diagram when they form a single phase or when two phases coexist [39, 65]. When Chol-analog spin labels are used, the DOT method can discriminate the l_o phase and the CBD [26, 68]. This case is described in this issue by Justyna Widomska et al.

Values of the OTP as a function of the overall Chol content for the DMPC/Chol bilayer at 27 °C (above the main phase transition temperature for the DMPC bilayer), measured close to the membrane surface with 5-PC and close to the membrane center with 14-PC, are shown in Fig. 6c. According to the phase diagram (Fig. 1), at an overall Chol content between 0 and ~ 10 mol%, the bilayer phase remains l_d (the Chol mole fraction in the l_d phase is the same as the experimental mixing ratio). Surprisingly, in the presence of Chol, the l_d phase exhibits higher OTP values across the entire membrane than without Chol. Variations of the overall Chol content between ~ 10 and ~ 30 mol% will affect the fractions of l_d and l_o phases. (It follows from Fig. 1 that, at 27 °C, each phase contains constant 6 and 27 mol% Chol, respectively.) In the l_o phase, the OTP's slight dependence on the overall Chol content in the range of ~ 10 to ~ 30 mol% for both 5-PC and 14-PC suggests that, in this Chol range, not only do changes of the relative amounts of l_d and l_o phases take place but also the size of the individual l_o-phase domain increases, reducing the effects of the surrounding l_d phases. With an overall Chol content between ~ 30 and 50%, the phase remains l_o. (The Chol mole fraction in the DMPC bilayer is the same as the experimental mixing ratio.) The major result for this Chol range is that the OTP profile in the l_o phase containing 50 mol% Chol differs dramatically from that in the phase containing 30 mol% Chol [39]. At 50 mol% Chol, the OTP in the bilayer center in the l_o phase is similar to that in the l_d phase without Chol, but the OTP near the membrane surface (up to the C9 carbon atom) is substantially smaller in the l_o phase (i.e., the Chol-based l_o phase is only ordered near the membrane surface, but it retains a high-level disorder in the bilayer center). This property may facilitate lateral mobility of small, lipid-soluble molecules even in the bilayer-ordered domains. As shown in the phase diagram (Fig. 1), at a Chol content greater than 50 mol%, CBDs are formed in the DMPC bilayer. In Fig. 6c, this is indicated by the values of the OTP obtained with ASL for a Chol content greater than 50 mol%. The DOT method with ASL not only discriminates CBDs formed within the l_o phase but also characterizes these two environments by the values of the OTP. At a Chol content greater than 66 mol% Chol, Chol crystals are formed. The OTP, measured using PL-analog spin labels located in the PL/Chol portion of the membrane, is not affected by the presence of CBDs formed within the Chol-saturated PL bilayer, nor by the Chol crystals formed presumably outside the membrane (Fig. 6c).

Discussion

Low Cholesterol Content

As follows from Figs 4b and c, 6b and c, bilayers in the liquid-disordered phase (without Chol or with a Chol

content below 10 mol%) are highly fluid at all depths. Interestingly, their fluidity, sensed by the mobility of molecular oxygen (Fig. 6c), is even enhanced by the presence of Chol. These bilayers also exhibit a moderate hydrophobic barrier (Fig. 5b and c). During evolution, PL membranes with a low Chol content were chosen to separate subcellular compartments as a nuclear envelope, membranes of rough and smooth endoplasmic reticulum, and membranes of Golgi apparatus.

The nuclear envelope, which is made of two lipid bilayers, separates the nucleus from the cytoplasm. It contains multiple pores that regulate the passage of macromolecules, such as proteins and RNA, between these two compartments but permit polar small molecules, such as water, ions, and ATP, to pass freely. Lipid bilayer membranes of rough endoplasmic reticulum provide the basic surface to which (on its outside surface) ribosomes are attached to synthetize specific proteins destined for secretion. These membranes are also involved in the intracellular transport of the products of the rough endoplasmic reticulum to the Golgi apparatus, where, after modification, proteins are packed into secretory vesicles and then transported to their destinations: lysosomes, the plasma membrane, or secretion. Smooth endoplasmic reticulum is devoted almost exclusively to the manufacture of lipids and steroid hormones. The l_d lipid bilayer membranes fulfill properties that are needed for these organelles to function properly. They form a physical, moderate hydrophobic barrier to keep genetic nucleus material separate from cytoplasm and to wrap macromolecules to form cargoes that can be safely transported through the cytoplasm. In the rough endoplasmic reticulum, they concentrate ribosomes (apparatus for protein synthesis) adjacent to the nucleus. It seems that a simple PL bilayer can provide the base for ribosome attachments.

Mitochondria membranes also belong to the low Chol content group. They are, however, involved in a very complex process of energy transduction. An electron transport chain located in the inner mitochondrial membrane, through a series of three proton pumps, creates the electrochemical proton gradient across the inner mitochondrial membrane [69]. The protons can return to the matrix through the ATP synthase complex, and their potential energy is used to synthesize ATP from ADP and inorganic phosphate. To make this process efficient, the proton leak across the lipid matrix of the inner mitochondrial membrane has to be minimized. Usually, membranes utilize Chol to create a high hydrophobic barrier, but Chol also strongly affects (decreases) membrane fluidity, which in this case is an undesirable effect. This problem was solved during evolution by loading the mitochondrial membranes with a highly unsaturated PL, cardiolipin [70–72]. As previously mentioned, polyunsaturated acyl chains of PLs create a high hydrophobic barrier across the bilayer, and, at the same time, prevent its high fluidity. In particular, elevated fluidity in mitochondrial membranes ensures the high mobility of CoQ_{10} within the bilayer, during its function as an electron carrier from enzyme complex I and enzyme complex II to enzyme complex III [8].

Normal Cholesterol Content

We classified membranes containing between 10 and 30 mol% Chol as those with a normal Chol content, as this range is typical for most plasma membranes. PL bilayer membranes with this Chol content possess unique lateral organization, namely coexisting l_d and l_o phases. Such organization is observed for membranes made both of a single PL species and of a mixture of PLs. The Chol-dependent l_o phase is attractive to researchers as it is connected to membrane microdomains, particularly so-called raft domains, or rafts. The interest in rafts spans a broad range of biomedical research areas related to cell-cell signaling and trafficking of lipids and proteins in cells [73–80]. Simons and Vaz [43] stated that, "rafts could be considered domains of a l_o phase." However, even though l_o and l_d phases are observed and measured in simple systems of model membranes, their concept cannot be directly applied to the living cell membranes. Nevertheless, it is likely that knowledge of how they form and their physico-chemical properties will contribute to our understanding of the formation mechanism, structure, lifetime, and dynamics of raft domains in biological membranes [67, 75, 78–83]. Results providing some insight into the structure and molecular interactions in l_o and l_d phases in PL bilayers are presented in Figs 3c, 4c, 5c, and 6c. (Look for Chol content between 10 and 30 mol% where properties of coexisting l_o and l_d phases are demonstrated.) These figures and our explanations show lateral segregation of the phases and also their depth-dependent properties; these indicate that the structure of the bilayers is nonuniform in three dimensions, which we refer to as the three-dimensional structure of the lipid bilayer [39, 75].

High Cholesterol Content

As follows from the phase diagram (Fig. 1), PL bilayers containing 30 to 50 mol% Chol form a single l_o phase. This Chol content is characteristic for plasma membranes of red blood cells and for myelin membranes of Schwann cells isolating nerve axons. This high Chol content ensures the highest hydrophobicity of the membrane as well as high membrane rigidity understood as reduced *trans-gauche* isomerization (extended conformation) and translational and rotational motion, e.g., ref. [84]. It should be noted that the properties of l_o-phase bilayers change significantly between 30 and 50 mol% Chol, as was shown using Chol-analog

spin labels [85] and PL-analog spin labels (discussed previously). The latter additionally shows that the three-dimensional dynamic structure of the bilayers differs significantly: At ~ 30 mol% Chol (the lowest Chol content of the l_o phase), the bell-shaped profile of the OTP is similar in shape (although shifted to lower values at all depths) to that for the l_d phase without Chol. At 50 mol% Chol (the highest Chol content of the single l_o phase), the profile becomes rectangular (Fig. 6b).

Incorporating saturating amounts of Chol into PL bilayers also ensures the rectangular shape of the hydrophobicity profile with the hydrophobicity in the bilayer center comparable to that of hexane ($\varepsilon = 2$) (Fig. 5b). This greatly increases the activation energy required for polar and small ionic molecules to pass through the membrane. Thus, the rate-limiting step for the permeability of small polar molecules is likely to be the process of crossing the hydrophobic barrier at the membrane center. Saturating amounts of Chol in the PL bilayer also creates resistance to the permeation of small hydrophobic molecules (like oxygen) across the membrane. As shown in Fig. 6b, a rather high permeability barrier to oxygen transport is located in the polar headgroup region, and in the hydrophobic core of the bilayer to the depth of the C9 carbon atom. Resistance to oxygen permeation in this region (we call it the "rigidity barrier") is much higher than resistance in the water phase. Thus, the rate-limiting step for permeation of small, nonpolar molecules across the membrane (including molecular oxygen) is likely to be the process of crossing the rigidity barrier located near the membrane surface.

Red blood cells (~ 8 μm in diameter) must withstand strong shear forces in the arteries, and must be able to fold up when they pass through narrow capillaries (<3 μm in diameter). To avoid any leakage of intracellular molecules, including hemoglobin, during these processes, the red blood cell plasma membrane must contain high (saturating) Chol concentrations. Additionally, because the red blood cell plasma membrane supported by the cytoskeleton is the only supramolecular structure of the cell (all intracellular organelles are absent), mainly integral membrane proteins are involved in regulatory processes maintaining appropriate conditions of the cytoplasm. For this reason, the membrane barrier must be very high to block nonspecific permeation of small molecules and to protect the cytoplasm. Incorporating a saturating amount of Chol into the membrane serves this purpose well, because Chol simultaneously raises hydrophobic barriers for polar molecules and increases rigidity barriers for nonpolar molecules. The question *Is the mammalian cell plasma membrane a barrier to oxygen transport?* is carefully discussed in [40, 86].

Similarly, the saturating Chol content in myelin membranes of Schwann cells ensures the highest electrical isolation of nerve axons and enables an especially rapid mode of electrical impulse propagation called saltatory conduction. To enhance insulating properties, these membranes contain high amounts of sphingolipids. Sphingolipids form tight links with Chol, which cause the membrane to become more compact (cf. [87]). Thus, axons are not only electrically shielded but also tightly isolated from being accessed by polar and nonpolar small molecules. Lipid composition and physico-chemical properties of myelin membranes are crucial because the membranes contain an amount of proteins (15–30% by weight) too small to be able to correct nonspecific leakage through the lipid.

Very High Cholesterol Content

The highest amount of Chol that can dissolve in a PL bilayer is 50 mol% (i.e., when the Chol/PL molar ratio is 1 [see schematic drawing in Fig. 1]). At a higher Chol/PL molar ratio, Chol is distributed between the Chol-saturated fraction of the PL/Chol bilayer and the CBDs immersed in it. Among biological membranes, such a high Chol content is observed only in the fiber cell plasma membranes of the eye lens, and this is their most unique biochemical characteristic. In the membrane of the human eye fiber cell, the Chol/PL molar ratio ranges from 1–2 in the lens cortex and can be as high as 3 to 4 in the lens nucleus (see sect. *Beyond the cholesterol solubility threshold*).

Based on the results of our EPR spin-labeling experiments with lens-lipid membranes as well as those found in the literature, we have been able to identify the functions of Chol specific to the fiber cell plasma membrane [10]. The CBD plays a crucial role in these membranes (again, we direct readers to this issue's article by Justyna Widomska et al. for more-detailed information) as it ensures that the surrounding PL bilayer is saturated with Chol. (See schematic drawing in Fig. 1.) CBDs start to form at 50 mol% Chol; an increase of the Chol content above 50 mol% does not change the properties of the surrounding PL bilayer (Figs 3c, 4c, 5c and 6c). This feature is independent of the bilayer PL composition as is clearly illustrated in Fig. 7, which shows profiles of the four measured properties across bilayers consisting of lipids obtained from human lens membranes from different donors. For all investigated age groups, appropriate profiles are identical.

One of the consequences of the unique growth pattern of the lens is that there is no protein turnover in the matured fiber cells [88, 89]. The lens proteins should perform the same functions in old lenses that they performed just after synthesis. The lack of protein turnover is seemingly in conflict with the drastic changes in the fiber cell membrane PL composition that occurs during aging [9, 27, 90–92]. Such changes would be expected to alter the functioning of membrane integral proteins. However, this is not the case; presented data indicate that the saturating Chol content in

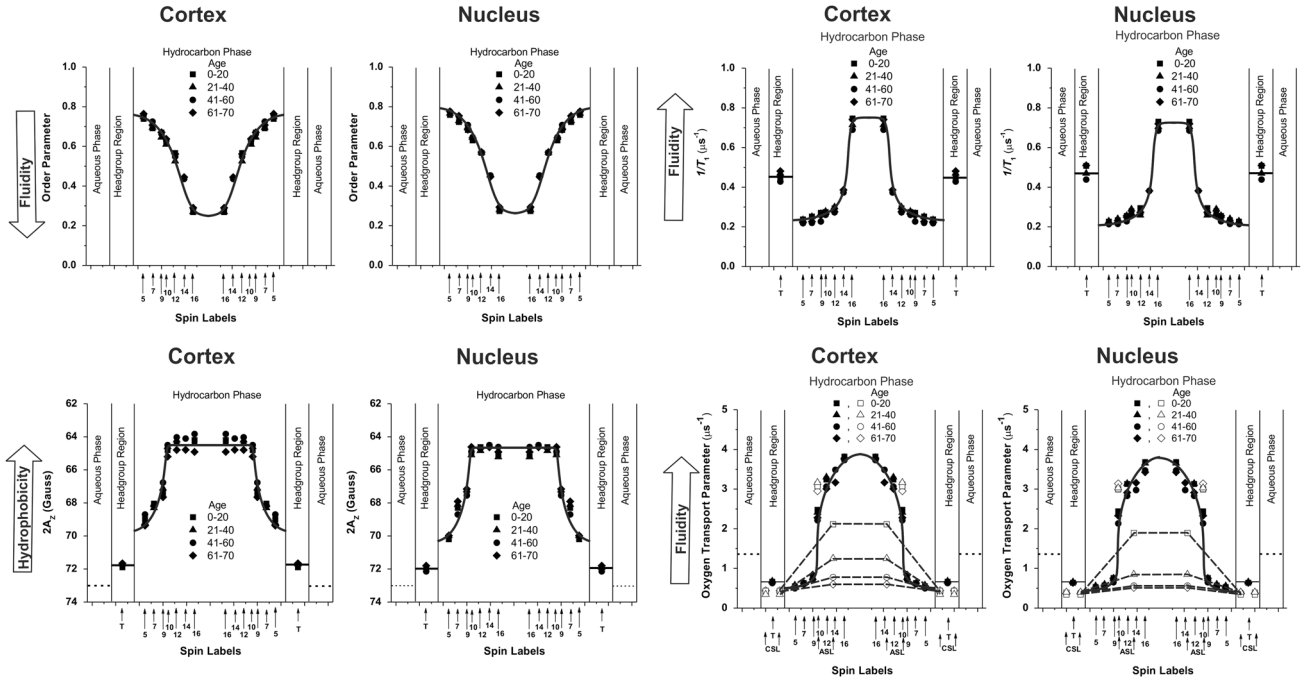

Fig. 7 Profiles of different membrane properties across lens lipid membranes of eye lenses from human donors of different age groups obtained using EPR spin labeling and approaches described in Figs 3–6. All profiles were obtained at 37 °C with the PL-analog spin labels. Data obtained with Chol-analog spin labels are included only into the profiles of the OTP. As indicated by profiles of the OTP (data obtained with ASL and CSL), the CBDs are present in membranes of all age groups, indicating that the surrounding PL bilayer is always saturated with Chol. Data for all age groups are reproduced from ref. [90], Copyright 2017, with permission from Taylor & Francis

these membranes (and the presence of CBDs) helps to maintain fiber cell membrane homeostasis during age-related changes of the PL composition without altering functions of integral proteins [11–14] and without compromising too much lens transparency. This constant saturating Chol content in the membranes of the fiber cells fulfills another important function as it makes the surfaces of the membrane smoother than otherwise. The smoother surface of each cell membrane reduces light scattering by the human lens and helps to maintain lens transparency [84].

Beyond The Cholesterol Solubility Threshold

When the Chol content in the membrane exceeds the CST, Chol crystals form; though it is not clear where this formation takes place, it most likely happens outside the membrane [30, 32]. As follows from sect. *Very high cholesterol content*, a high Chol content and CBDs serve beneficial functions for eye lenses. Can we also call formation of Chol crystals beneficial? Probably not. Our results indicate, however, that formation of Chol crystals is not harmful for aged human lenses [93]. Formation of Chol crystals in other tissues and organs is a sign of pathology. It was shown that deposition of the minute Chol crystals found in artery cells can initiate and promote atherosclerosis by activating inflammasomes [94] and, in fact, is an early cause of atherosclerosis. Some possible pathways lead to the formation of Chol crystals in the artery. One pathway that already has been investigated is the uptake of oxidized low density lipoproteins by macrophages, which promotes the intracellular accumulation of free Chol and the formation of Chol crystals, inflammation, and disease [30]. The alternative pathway involves plasma membranes oversaturated with Chol. This pathway should be very efficient in aged fiber cell membranes where Chol crystals already were detected [30, 31, 95]. However, inflammation does not appear to play a role in cataract formation. The unique structure of the lens protects it from the harmful induction of inflammasomes, as mature fiber cells do not contain intracellular organelles, and from initiation of the inflammatory cascade, as the lens is avascular. Thus, Chol crystals can be formed without harmful effects on lens properties (clarity) and functions. All these factors suggest that high Chol content, formation of CBDs, and formation of Chol crystals should not be considered major predispositions for the development of age-related cataracts [93].

Concluding Remarks

The role of Chol in the biological membrane is a long-standing puzzle. Kusumi et al. [96] first introduced the

expression "fluidity buffer," stating that "cholesterol acts as a 'fluidity buffer' so that small changes in the amount and arrangement of membrane proteins may not affect the overall properties of the membranes." Later, he and the co-authors proposed that the membrane mixture of saturated and unsaturated acyl chains of PLs with Chol also provides a fluidity buffer [97, 98]. Present results suggest that Chol also has other crucial functions specific to certain biological membranes. At different Chol contents, the effects of Chol on the membrane properties (fluidity, permeability) and organization (phase and domain formation) are very different. We would like to conclude this review with a few remarks about findings that have emerged from our EPR spin-labeling studies of lipid and biological membranes supported in some places by our molecular modeling studies.

Ordering Effects of Cholesterol

The ordering effect of Chol in saturated PC bilayers is very strong. The acyl chain order parameter, when plotted as a function of the mole fraction of Chol at the same temperature above the main phase transition temperature of a PC bilayer with saturated chains of 14–22 carbon atoms, is nearly the same for all PC bilayers. This occurs over a wide range of temperatures and Chol mole fractions [97]. Chol also strongly reduces the rotational and wobbling motion of saturated acyl chains [48]. Unsaturated acyl chains greatly reduce these Chol effects, e.g., [99], thus allowing us to make the following final conclusion: The "fluidizing" effect of unsaturated chains observed in biological membranes seems to manifest itself by moderating the "rigidifying" effect of Chol.

Hydrophobic Barrier Formed by Acyl Chain Unsaturation and Cholesterol

Since cellular plasma membranes face the cell's external environment, the membrane barriers must be very high to block nonspecific permeation of small molecules. Incorporation of Chol into the membrane serves this purpose well, because Chol simultaneously raises hydrophobic barriers for polar molecules and increases rigidity barriers for nonpolar molecules. The locations of permeation barriers are different for polar and nonpolar molecules. For the former, the major resistance to permeation is the hydrophobic barrier in the central part of the membrane. For the latter, the major resistance to permeation is the rigidity barrier near the membrane surface.

Pure saturated PC bilayers (without Chol) exhibit low hydrophobicity across the bilayer; at the bilayer center, where hydrophobicity is the highest, it is comparable to that of propanol and octanol ($\varepsilon = 10$–20) [59]. Introduction of a double bond to the acyl chain does increase bilayer hydrophobicity at all locations. This effect is especially great for the cis conformation of the double bond, for which hydrophobicity in the bilayer center increases to the level of dipropylamine ($\varepsilon = 3$, dioleoylphosphatidylcholine, DOPC) [59]. This suggests that the lipid-bilayer portion of the biological membrane can be a significant hydrophobic barrier only when it includes unsaturated acyl chains and/or Chol. Nature sometimes replaces Chol with polyunsaturated PLs to create membranes with a high hydrophobic barrier, especially when prevention of high membrane fluidity was necessary.

Hydrophobic Channeling

The striking similarity between the OTP (like in Fig. 6b) and hydrophobicity (like in Fig. 5b) profiles, especially for PL bilayers saturated with Chol, suggests a possibility for lateral transport of molecular oxygen and other small, nonpolar molecules in the central region of the membrane (parallel to the membrane surface), which we named "hydrophobic channeling." This hypothesis was first formulated by Skulachev [100] for the transport of small hydrophobic solutes within the cell using extended membranous systems. The resistance to the movement of oxygen and other small, hydrophobic molecules in the membrane center is much lower than in the water phase, whereas their solubility is much higher. To escape from these channels, they have to cross high barriers with low permeability existing on both sides of the membrane (see ref. [101] for more explanation). This supports our hypothesis that a high Chol membrane content is responsible for creating hydrophobic channels for the movement of small, hydrophobic molecules, and, at the same time, it is responsible for creating the rigidity barrier to transport these molecules across the membrane.

Fluid-Phase Microimmiscibility of Unsaturated Phospholipids and Cholesterol

EPR spin-labeling measurements indicated that, in the DOPC/Chol bilayer, Chol is segregated from the bulk DOPC phase, forming Chol-enriched domains or clustered Chol domains, due to the structural conflict between the rigid ring skeleton of Chol and the rigid bend of the C9–C10 cis double bond in each DOPC acyl chain. However, such a domain is small and likely to consist of only several Chol molecules, and it is short lived, of the order of 1–100 ns [38]. The following two points are our speculations: (1) In a biological membrane, which, in general, contains both saturated and unsaturated PLs, Chol-enriched domains may be stabilized by the presence of the saturated acyl chains of sphingomyelin, and also by the clustered raft

proteins. In the influenza viral membrane, one of the simplest forms of a biological membrane, the lifetime of a protein-rich, Chol-rich domain was found to be of the order of 100 μs [67], again showing the small/unstable nature of rafts in unstimulated cells. (2) At variance with the general view (e.g., ref. [5]), the formation of rafts may not be due to the affinity of Chol and saturated acyl chains, but rather to the segregation of Chol from the liquid-crystalline unsaturated bulk-phase membrane. Saturated PL chains may be associated with both the Chol-enriched domains and the disordered bulk domain, optimizing both structures such as to obtain the free energy minimum (possibly local and temporal minimum) of the whole membrane (see [75] for more discussion).

Properties of The Liquid-Ordered Phase

Additionally, data obtained with EPR spectroscopy of spin-labels attached to PL acyl chains at specific depths and located in specific membrane domains allowed correcting the commonly accepted statement that the properties of the l_o-phase domains are between those for the l_d and s_o domains [102]. This statement is true for membranes containing bulk Chol mole fractions below 30%, where the l_o domain coexists with the l_d or s_o domain (see Fig. 1). However, at a higher Chol content, even though the membrane is in the l_o phase, the OTP in the region near the membrane surface (from the surface to the depth of the C9 carbon atom) is like that in the s_o phase, and in the central region of the membrane (at depths greater than that of the C9 carbon atom), it is like that in the l_d phase.

Understanding Cholesterol's Functions in Model Membranes Helps To Understand Its Functions in Biological Membranes

In our opinion, the amount of data collected for simple lipid bilayers and those made from total lipid extracts of biological membranes is sufficient to determine some significant functions of Chol specific to the biological membranes discussed above. We are aware of the limitations of the conclusions and hypotheses presented in this review, as the membranes studied by us do not contain proteins. Intact membranes are sometimes loaded with membrane proteins, which raises questions and concerns regarding extent to which the presented conclusions can apply. Nevertheless, the study of the functions of Chol in simple models is undoubtedly helpful to better understanding its functions in intact membranes. Also, it is indispensable in revealing the mechanisms by which intrinsic proteins affect the properties of the lipid-bilayer portion of a biological membrane. Additionally, in this review, we directed the readers' attention to profiles of physical properties across membranes saturated and oversaturated with Chol, which have filled an existing gap in membrane research.

Acknowledgements This work was supported by grants EY015526, EB001980, and EY001931 from the National Institutes of Health, USA. Faculty of Biochemistry, Biophysics, and Biotechnology of Jagiellonian University is a partner of the Leading National Research Center (KNOW) supported by the Ministry of Science and Higher Education, Poland.

Conflict of Interest The authors declare that they have no competing interests.

References

1. Roux, B., Berneche, S., Egwolf, B., Lev, B., Noskov, S. Y., Rowley, C. N., et al. (2011). Ion selectivity in channels and transporters. *The Journal of General Physiology*, *137*, 415–426.
2. Hille, B. (2001). *Ion Channels of Excitable Membranes*. (3rd Edition). Sinauer Associates Inc, Sunderland, MA.
3. Luckey, M. (2008). *Membrane Structural Biology: with Biochemical and Biophysical Foundations*. Cambridge University Press, New York, NY.
4. Diamond, J. M., & Katz, Y. (1974). Interpretation of nonelectrolyte partition coefficients between dimyristoyl lecithin and water. *Journal of Membrane Biology*, *17*, 121–154.
5. Viola, A. (2001). The amplification of TCR signaling by dynamic membrane microdomains. *Trends in Immunology*, *22*, 322–327.
6. Simons, K., & Toomre, D. (2000). Lipid rafts and signal transduction. *Nature Reviews. Molecular Cell Biology*, *1*, 31–39.
7. Kusumi, A., Fujiwara, T. K., Morone, N., Yoshida, K. J., Chadda, R., Xie, M., et al. (2012). Membrane mechanisms for signal transduction: the coupling of the meso-scale raft domains to membrane-skeleton-induced compartments and dynamic protein complexes. *Seminars in Cell and Developmental Biology*, *23*, 126–144.
8. Nelson, D. L., & Cox, M. M. (2008). *Lehninger Principles of Biochemistry*. 5th edition. W. H. Freeman and Company, New York, NY.
9. Borchman, D., & Yappert, M. C. (2010). Lipids and the ocular lens. *Journal of Lipid Research*, *51*, 2473–2488.
10. Subczynski, W. K., Raguz, M., Widomska, J., Mainali, L., & Konovalov, A. (2012). Functions of cholesterol and the cholesterol bilayer domain specific to the fiber-cell plasma membrane of the eye lens. *Journal of Membrane Biology*, *245*, 51–68.
11. Epand, R. M. (2005). Role of membrane lipids in modulating the activity of membrane-bound enzymes. In P. L. Yeagle (Ed.), *The Structure of Biological Membrane* (pp. 499–509). Boca Raton: CRC Press.
12. Reichow, S. L., & Gonen, T. (2009). Lipid-protein interactions probed by electron crystallography. *Current Opinion in Structural Biology*, *19*, 560–565.
13. Tong, J., Briggs, M. M., & McIntosh, T. J. (2012). Water permeability of aquaporin-4 channel depends on bilayer composition, thickness, and elasticity. *Biophysical Journal*, *103*, 1899–1908.
14. Tong, J., Canty, J. T., Briggs, M. M., & McIntosh, T. J. (2013). The water permeability of lens aquaporin-0 depends on its lipid bilayer environment. *Experimental Eye Research*, *113*, 32–40.
15. Bloch, K. E. (1983). Sterol structure and membrane function. *CRC Critical Reviews in Biochemistry*, *14*, 47–92.

16. Bloom, M., & Mouritsen, O. G. (1995). The evolution of membrane. In R. Lipowsky, E. Sackmann (eds.). *Structure and Dynamics of Membrane* (pp. 65–95). Amsterdam: Elsevier.
17. Miao, L., Nielsen, M., Thewalt, J., Ipsen, J. H., Bloom, M., Zuckermann, M. J., et al. (2002). From lanosterol to cholesterol: structural evolution and differential effects on lipid bilayers. *Biophysical Journal*, *82*, 1429–1444.
18. Rog, T., Pasenkiewicz-Gierula, M., Vattulainen, I., & Karttunen, M. (2007). What happens if cholesterol is made smoother: importance of methyl substituents in cholesterol ring structure on phosphatidylcholine-sterol interaction. *Biophysical Journal*, *92*, 3346–3357.
19. Hannich, J. T., Umebayashi, K., & Riezman, H. (2011). Distribution and functions of sterols and sphingolipids. *Cold Spring Harbor Perspectives in Biology*, *3*, 1–14.
20. Bretscher, M. S., & Munro, S. (1993). Cholesterol and the Golgi apparatus. *Science (New York, N.Y.)*, *261*, 1280–1281.
21. Schroeder, F., Frolov, A. A., Murphy, E. J., Atshaves, B. P., Jefferson, J. R., Pu, L., et al. (1996). Recent advances in membrane cholesterol domain dynamics and intracellular cholesterol trafficking. *Proceedings of the Society for Experimental Biology and Medicine. Society for Experimental Biology and Medicine*, *213*, 150–177.
22. van Meer, G., Voelker, D. R., & Feigenson, G. W. (2008). Membrane lipids: where they are and how they behave. *Nature reviews. Molecular Cell Biology*, *9*, 112–124.
23. Spector, A. A., & Yorek, M. A. (1985). Membrane lipid composition and cellular function. *Journal of Lipid Research*, *26*, 1015–1035.
24. Shinitzky, M., & Barenholz, Y. (1978). Fluidity parameters of lipid regions determined by fluorescence polarization. *Biochimica et Biophysica Acta*, *515*, 367–394.
25. Mainali, L., Raguz, M., & Subczynski, W. K. (2013). Formation of cholesterol bilayer domains precedes formation of cholesterol crystals in cholesterol/dimyristoylphosphatidylcholine membranes: EPR and DSC studies. *Journal of Physical Chemistry B*, *117*, 8994–9003.
26. Raguz, M., Mainali, L., Widomska, J., & Subczynski, W. K. (2011). Using spin-label electron paramagnetic resonance (EPR) to discriminate and characterize the cholesterol bilayer domain. *Chemistry and Physics of Lipids*, *164*, 819–829.
27. Li, L. K., So, L., & Spector, A. (1987). Age-dependent changes in the distribution and concentration of human lens cholesterol and phospholipids. *Biochimica et Biophysica Acta*, *917*, 112–120.
28. Truscott, R. J. (2000). Age-related nuclear cataract: a lens transport problem. *Ophthalmic Research*, *32*, 185–194.
29. Li, L. K., So, L., & Spector, A. (1985). Membrane cholesterol and phospholipid in consecutive concentric sections of human lenses. *Journal of Lipid Research*, *26*, 600–609.
30. Mason, R. P., & Jacob, R. F. (2003). Membrane microdomains and vascular biology. Emerging role in atherogenesis. *Circulation*, *107*, 2270–2273.
31. Mason, R., Tulenko, T. N., & Jacob, R. F. (2003). Direct evidence for cholesterol crystalline domains in biological membranes: role in human pathobiology. *Biochimica et Biophysica Acta*, *1610*, 198–207.
32. Jacob, R. F., Cenedella, R. J., & Mason, R. P. (1999). Direct evidence for immiscible cholesterol domains in human ocular lens fiber cell plasma membranes. *Journal of Biological Chemistry*, *274*, 31613–31618.
33. Singer, S. J., & Nicolson, G. L. (1972). The fluid mosaic model of the structure of cell membranes. *Science (New York, N.Y.)*, *175*, 720–731.
34. Kusumi, A., Suzuki, K. G., Kasai, R. S., Ritchie, K., & Fujiwara, T. K. (2011). Hierarchical mesoscale domain organization of the plasma membrane. *Trends in Biochemical Sciences*, *36*, 604–615.
35. Kusumi, A., Fujiwara, T. K., Chadda, R., Xie, M., Tsunoyama, T. A., Kalay, Z., et al. (2012). Dynamic organizing principles of the plasma membrane that regulate signal transduction: commemorating the fortieth anniversary of Singer and Nicolson's fluid-mosaic model. *Annual Review of Cell and Developmental Biology*, *28*, 215–250.
36. Wisniewska, A., Draus, J., & Subczynski, W. K. (2003). Is a fluid-mosaic model of biological membranes fully relevant? Studies on lipid organization in model and biological membranes. *Cellular and Molecular Biology Letters*, *8*, 147–159.
37. Nicolson, G. L. (2014). The fluid-mosaic model of membrane structure: still relevant to understanding the structure, function and dynamics of biological membranes after more than 40 years. *Biochimica et Biophysica Acta*, *1838*, 1451–1466.
38. Subczynski, W. K., Antholine, W. E., Hyde, J. S., & Kusumi, A. (1990). Microimmiscibility and three-dimensional dynamic structures of phosphatidylcholine-cholesterol membranes: translational diffusion of a copper complex in the membrane. *Biochemistry*, *29*, 7936–7945.
39. Subczynski, W. K., Wisniewska, A., Hyde, J. S., & Kusumi, A. (2007). Three-dimensional dynamic structure of the liquid-ordered domain in lipid membranes as examined by pulse-EPR oxygen probing. *Biophysical Journal*, *92*, 1573–1584.
40. Subczynski, W. K., Hyde, J. S., & Kusumi, A. (1991). Effect of alkyl chain unsaturation and cholesterol intercalation on oxygen transport in membranes: a pulse ESR spin labeling study. *Biochemistry*, *30*, 8578–8590.
41. Almeida, P. F., Pokorny, A., & Hinderliter, A. (2005). Thermodynamics of membrane domains. *Biochimica et Biophysica Acta*, *1720*, 1–13.
42. Heberle, F. A., & Feigenson, G. W. (2011). Phase separation in lipid membranes. *Cold Spring Harbor. Perspectives in Biology*, *3*, 1–13.
43. Simons, K., & Vaz, W. L. (2004). Model systems, lipid rafts, and cell membranes. *Annual Review of Biophysics and Biomolecular Structure*, *33*, 269–295.
44. Huang, J., Buboltz, J. T., & Feigenson, G. W. (1999). Maximum solubility of cholesterol in phosphatidylcholine and phosphatidylethanolamine bilayers. *Biochimica et Biophysica Acta*, *1417*, 89–100.
45. Marsh, D. (1981). Electron spin resonance: spin labels. In E. Grell (ed.), *Membrane Spectroscopy* (pp. 51–142). Berlin: Springer.
46. Devaux, P. F. (1983). ESR and NMR studies of lipid-protein interactions in membranes. In L. J. Berliner, J. Reuben (eds.), *Biological Magnetic Resonance* (pp. 183–299). New York: Plenum Press.
47. Schreier, S., Polnaszek, C. F., & Smith, I. C. (1978). Spin labels in membranes. Problems in practice. *Biochimica et Biophysica Acta*, *515*, 395–436.
48. Rog, T., & Pasenkiewicz-Gierula, M. (2001). Cholesterol effects on the phosphatidylcholine bilayer nonpolar region: a molecular simulation study. *Biophysical Journal*, *81*, 2190–2202.
49. Mainali, L., Feix, J. B., Hyde, J. S., & Subczynski, W. K. (2011). Membrane fluidity profiles as deduced by saturation-recovery EPR measurements of spin-lattice relaxation times of spin labels. *Journal of Magnetic Resonance*, *212*, 418–425.
50. Mainali, L., Hyde, J. S., & Subczynski, W. K. (2013). Using spin-label W-band EPR to study membrane fluidity profiles in samples of small volume. *Journal of Magnetic Resonance*, *226*, 35–44.
51. Robinson, B. H., Haas, D. A., & Mailer, C. (1994). Molecular dynamics in liquids: spin-lattice relaxation of nitroxide spin labels. *Science (New York, N.Y.)*, *263*, 490–493.

52. Mailer, C., Nielsen, R. D., & Robinson, B. H. (2005). Explanation of spin-lattice relaxation rates of spin labels obtained with multifrequency saturation recovery EPR. *The Journal of Physical Chemistry. A*, *109*, 4049–4061.
53. Rog, T., & Pasenkiewicz-Gierula, M. (2004). Non-polar interactions between cholesterol and phospholipids: a molecular dynamics simulation study. *Biophysical Chemistry*, *107*, 151–164.
54. Rog, T., & Pasenkiewicz-Gierula, M. (2001). Cholesterol effects on the phospholipid condensation and packing in the bilayer: a molecular simulation study. *FEBS Letters*, *502*, 68–71.
55. Murzyn, K., Rog, T., Jezierski, G., Takaoka, Y., & Pasenkiewicz-Gierula, M. (2001). Effects of phospholipid unsaturation on the membrane/water interface: a molecular simulation study. *Biophysical Journal*, *81*, 170–183.
56. Plesnar, E., Subczynski, W. K., & Pasenkiewicz-Gierula, M. (2013). Comparative computer simulation study of cholesterol in hydrated unary and binary lipid bilayers and in an anhydrous crystal. *The Journal of Physical Chemistry. B*, *117*, 8758–8769.
57. Griffith, O. H., Dehlinger, P. J., & Van, S. P. (1974). Shape of the hydrophobic barrier of phospholipid bilayers (evidence for water penetration in biological membranes). *Journal of Membrane Biology*, *15*, 159–192.
58. Griffith, O. H., & Jost, P. C. (1976). Lipid spin labels in biological membranes. In L. J. Berliner (ed.), *Spin Labeling Theory and Applications* (pp. 453–523). New York, San Francisco, London: Academic Press.
59. Subczynski, W. K., Wisniewska, A., Yin, J.-J., Hyde, J. S., & Kusumi, A. (1994). Hydrophobic barriers of lipid bilayer membranes formed by reduction of water penetration by alkyl chain unsaturation and cholesterol. *Biochemistry*, *33*, 7670–7681.
60. Wisniewska, A., & Subczynski, W. K. (1998). Effects of polar carotenoids on the shape of the hydrophobic barrier of phospholipid bilayers. *Biochimica et Biophysica Acta*, *1368*, 235–246.
61. Kusumi, A., Subczynski, W. K., & Hyde, J. S. (1982). Oxygen transport parameter in membranes as deduced by saturation recovery measurements of spin-lattice relaxation times of spin labels. *Proceedings of National Academic Sciences USA*, *79*, 1854–1858.
62. Subczynski, W. K., Hyde, J. S., & Kusumi, A. (1989). Oxygen permeability of phosphatidylcholine-cholesterol membranes. *Proceedings National Academic Sciences USA*, *86*, 4474–4478.
63. Ashikawa, I., Yin, J.-J., Subczynski, W. K., Kouyama, T., Hyde, J. S., & Kusumi, A. (1994). Molecular organization and dynamics in bacteriorhodopsin-rich reconstituted membranes: discrimination of lipid environments by the oxygen transport parameter using a pulse ESR spin-labeling technique. *Biochemistry*, *33*, 4947–4952.
64. Subczynski, W. K., Widomska, J., Wisniewska, A., & Kusumi, A. (2007). Saturation-recovery electron paramagnetic resonance discrimination by oxygen transport (DOT) method for characterizing membrane domains. In T. J. McIntosh (Ed.) *Methods in Molecular Biology, Lipid Rafts* (pp. 143–157). Humana Press: Totowa.
65. Mainali, L., Raguz, M., & Subczynski, W. K. (2011). Phase-separation and domain-formation in cholesterol-sphingomyelin mixture: pulse-EPR oxygen probing. *Biophysical Journal*, *101*, 837–846.
66. Subczynski, W. K., Raguz, M., & Widomska, J. (2010). Studying lipid organization in biological membranes using liposomes and EPR spin labeling. *Methods in Molecular Biology*, *606*, 247–269.
67. Kawasaki, K., Yin, J.-J., Subczynski, W. K., Hyde, J. S., & Kusumi, A. (2001). Pulse EPR detection of lipid exchange between protein rich raft and bulk domains in the membrane: methodology development and its application to studies of influenza viral membrane. *Biophysical Journal*, *80*, 738–748.
68. Raguz, M., Mainali, L., Widomska, J., & Subczynski, W. K. (2011). The immiscible cholesterol bilayer domain exists as an integral part of phospholipid bilayer membranes. *Biochimica et Biophysica Acta*, *1808*, 1072–1080.
69. Mitchell, P. (1961). Coupling of phosphorylation to electron and hydrogen transfer by a chemi-osmotic type of mechanism. *Nature*, *191*, 144–148.
70. Mannella, C. A. (2006). Structure and dynamics of the mitochondrial inner membrane cristae. *Biochimica et Biophysica Acta*, *1763*, 542–548.
71. Schlame, M., Brody, S., & Hostetler, K. Y. (1993). Mitochondrial cardiolipin in diverse eukaryotes. Comparison of biosynthetic reactions and molecular acyl species. *European Journal of Biochemistry*, *212*, 727–735.
72. Schlame, M., Horvath, L., & Vigh, L. (1990). Relationship between lipid saturation and lipid-protein interaction in liver mitochondria modified by catalytic hydrogenation with reference to cardiolipin molecular species. *The Biochemical Journal*, *265*, 79–85.
73. Simons, K., & Ikonen, E. (1997). Functional rafts in cell membranes. *Nature*, *387*, 569–572.
74. Zurzolo, C., van Meer, G., & Mayor, S. (2003). The order of rafts. Conference on microdomains, lipid rafts and caveolae. *EMBO Reports*, *4*, 1117–1121.
75. Subczynski, W. K., & Kusumi, A. (2003). Dynamics of raft molecules in the cell and artificial membranes: approaches by pulse EPR spin labeling and single molecule optical microscopy. *Biochimica et Biophysica Acta*, *1610*, 231–243.
76. Mayor, S., & Rao, M. (2004). Rafts: scale-dependent, active lipid organization at the cell surface. *Traffic (Copenhagen, Denmark)*, *5*, 231–240.
77. Mukherjee, S., & Maxfield, F. R. (2004). Membrane domains. *Annual Review of Cell and Developmental Biology*, *20*, 839–866.
78. Kusumi, A., Koyama-Honda, I., & Suzuki, K. (2004). Molecular dynamics and interactions for creation of stimulation-induced stabilized rafts from small unstable steady-state rafts. *Traffic (Copenhagen, Denmark)*, *5*, 213–230.
79. Kusumi, A., Nakada, C., Ritchie, K., Murase, K., Suzuki, K., Murakoshi, H., et al. (2005). Paradigm shift of the plasma membrane concept from the two-dimensional continuum fluid to the partitioned fluid: high-speed single-molecule tracking of membrane molecules. *Annual Review of Biophysics and Biomolecular Structure*, *34*, 351–378.
80. Kusumi, A., Ike, H., Nakada, C., Murase, K., & Fujiwara, T. (2005). Single-molecule tracking of membrane molecules: plasma membrane compartmentalization and dynamic assembly of raft-philic signaling molecules. *Seminars in Immunology*, *17*, 3–21.
81. Munro, S. (2003). Lipid rafts: elusive or illusive? *Cell*, *115*, 377–388.
82. Taner, S. B., Onfelt, B., Pirinen, N. J., McCann, F. E., Magee, A. I., & Davis, D. M. (2004). Control of immune responses by trafficking cell surface proteins, vesicles and lipid rafts to and from the immunological synapse. *Traffic (Copenhagen, Denmark)*, *5*, 651–661.
83. van Meer, G., & Sprong, H. (2004). Membrane lipids and vesicular traffic. *Current Opinion in Cell Biology*, *16*, 373–378.
84. Plesnar, E., Subczynski, W. K., & Pasenkiewicz-Gierula, M. (2012). Saturation with cholesterol increases vertical order and smoothes the surface of the phosphatidylcholine bilayer: a molecular simulation study. *Biochimica et Biophysica Acta*, *1818*, 520–529.
85. Kusumi, A., & Pasenkiewicz-Gierula, M. (1988). Rotational diffusion of a steroid molecule in phosphatidylcholine

membranes: effects of alkyl chain length, unsaturation, and cholesterol as studied by a spin-label method. *Biochemistry*, *27*, 4407–4415.
86. Subczynski, W. K., Hopwood, L. E., & Hyde, J. S. (1992). Is the mammalian cell plasma membrane a barrier to oxygen transport? *Journal of General Physiology*, *100*, 69–87.
87. Rog, T., & Pasenkiewicz-Gierula, M. (2006). Cholesterol-sphingomyelin interactions: a molecular dynamics simulation study. *Biophysical Journal*, *91*, 3756–3767.
88. Harding, J. J. (1997). Biochemistry of the eye. In J. J. Harding (Ed.), *Lens* (pp. 94–135). London: Chapman and Hall.
89. Lynnerup, N., Kjeldsen, H., Heegaard, S., Jacobsen, C., & Heinemeier, J. (2008). Radiocarbon dating of the human eye lens crystallines reveal proteins without carbon turnover throughout life. *PloS One*, *3*, e1529.
90. Mainali, L., Raguz, M., O'Brien, W.J., & Subczynski, W.K. (2016). Changes in the properties and organization of human lens lipid membranes occurring with age. *Current Eye Research*, doi:10.1080/02713683.02712016.01231325.
91. Yappert, M. C., Rujoi, M., Borchman, D., Vorobyov, I., & Estrada, R. (2003). Glycero- versus sphingo-phospholipids: correlations with human and non-human mammalian lens growth. *Experimental Eye Research*, *76*, 725–734.
92. Rujoi, M., Jin, J., Borchman, D., Tang, D., & Yappert, M. C. (2003). Isolation and lipid characterization of cholesterol-enriched fractions in cortical and nuclear human lens fibers. *Investigative Ophthalmology and Visual Science*, *44*, 1634–1642.
93. Mainali, L., Raguz, M., O'Brien, W. J., & Subczynski, W. K. (2015). Properties of membranes derived from the total lipids extracted from clear and cataractous lenses of 61-70-year-old human donors. *European Biophysics Journal*, *44*, 91–102.
94. Duewell, P., Kono, H., Rayner, K. J., Sirois, C. M., Vladimer, G., Bauernfeind, F. G., et al. (2010). NLRP3 inflammasomes are required for atherogenesis and activated by cholesterol crystals. *Nature*, *464*, 1357–1361.
95. Jacob, R. F., Cenedella, R. J., & Mason, R. P. (2001). Evidence for distinct cholesterol domains in fiber cell membranes from cataractous human lenses. *Journal of Biological Chemistry*, *276*, 13573–13578.
96. Kusumi, A., Tsuda, M., Akino, T., Ohnishi, S., & Terayama, Y. (1983). Protein-phospholipid-cholesterol interaction in the photolysis of invertebrate rhodopsin. *Biochemistry*, *22*, 1165–1170.
97. Kusumi, A., Subczynski, W. K., Pasenkiewicz-Gierula, M., Hyde, J. S., & Merkle, H. (1986). Spin-label studies on phosphatidylcholine-cholesterol membranes: effects of alkyl chain length and unsaturation in the fluid phase. *Biochimica et Biophysica Acta*, *854*, 307–317.
98. Subczynski, W. K., & Wisniewska, A. (2000). Physical properties of lipid bilayer membranes: relevance to membrane biological functions. *Acta Biochimica Polonica*, *47*, 613–625.
99. Rog, T., & Pasenkiewicz-Gierula, M. (2006). Cholesterol effects on a mixed-chain phosphatidylcholine bilayer: a molecular dynamics simulation study. *Biochimie*, *88*, 449–460.
100. Skulachev, V. P. (1990). Power transmission along biological membranes. *Journal of Membrane Biology*, *114*, 97–112.
101. Raguz, M., Widomska, J., Dillon, J., Gaillard, E. R., & Subczynski, W. K. (2009). Physical properties of the lipid bilayer membrane made of cortical and nuclear bovine lens lipids: EPR spin-labeling studies. *Biochimica et Biophysica Acta*, *1788*, 2380–2388.
102. Loura, L. M., Fedorov, A., & Prieto, M. (2001). Fluid-fluid membrane microheterogeneity: a fluorescence resonance energy transfer study. *Biophysical Journal*, *80*, 776–788.